UTILIZATION OF FOURIER TRANSFORM INFRARED ON MICROSTRUCTURAL EXAMINATION OF SFC NO-CEMENT BINDER
ỨNG DỤNG KỸ THUẬT QUANG PHỔ CHUYỂN ĐỔI HỒNG NGOẠI TRONG VIỆC XÁC ĐỊNH VI KẾT CẤU CỦA CHẤT KẾT DÍNH SFC KHÔNG XI MĂNG

Hoang-Anh Nguyen[1], Vu-An Tran[1], Duy-Hai Vo[2]

[1]*Can Tho University; hoanganh@ctu.edu.vn, tranvuan@ctu.edu.vn*
[2]*The University of Danang, University of Technology and Education; duyhai88@gmail.com*

Abstract - The research aims at proposing an innovative application of using Fourier transform infrared (FTIR) to examine the microstructure of a new no-cement SFC binder paste, which is fabricated with mixture of ground granulated blast furnace slag (GGBFS). Type F fly ash, and circulating fluidized bed combustion (CFBC) fly ash.15% CFA is used as the main activator to trigger the hydration of various mixtures of GGBFS and FFA. The results show that CFA mainly consists of portlandite ($Ca(OH)_2$) and anhydrite ($CaSO_4$) which attributes to the hydraulic property of SFC powder. The main hydration products of the hardened paste are ettringite (AFt) and calcium aluminum silicate hydrate (C-A-S-H) gel. An increase in FFA addition leads to the higher degree of AFt precipitation induced by an increase of active alumina.

Key words - CFBC fly ash; low calcium fly ash; slag; no-cement binder; Fourier transform infrared (FTIR).

Tóm tắt - Mục đích của nghiên cứu hiện tại nhằm đề nghị sử dụng kỹ thuật quang phổ chuyển đổi hồng ngoại (FTIR) cho việc phân tích vi cấu trúc của hỗn hợp vữa chất kết dính không xi măng SFC vốn được chế tạo từ 100% hỗn hợp phế phẩm công nghiệp gồm xỉ lò cao (GGBFS), tro bay loại canxi thấp (FFA), và hoạt chất từ phế phẩm tro bay từ công nghệ khử lưu huỳnh (CFA). Kết quả nghiên cứu chỉ ra rằng CFA chủ yếu được cấu thành từ canxi hydroxit ($Ca(OH)_2$) và thạch cao khan ($CaSO_4$) góp phần chính yếu quyết định tính chất thủy hóa của hỗn hợp vữa. Sản phẩm thủy hóa chủ yếu của hỗn hợp vữa bao gồm ettringite (AFt) và chất keo dính calcium aluminum silicate hydrate (C-A-S-H). Tăng hàm lượng FFA làm tăng hàm lượng alumina và dẫn đến tăng hàm lượng sản phẩm thủy hóa Aft.

Từ khóa - Tro bay CFBC; tro bay canxi thấp; xỉ lò cao; chất kết dính không xi măng; quang phổ chuyển đổi hồng ngoại (FTIR).

1. Introduction

ordinary Portland cement (OPC) because ucture consumes embodied energy much lower than metal materials such as steel or aluminum [1]. But a great deal of CO_2g the OPC manufacture impact on. [1Moreover, the OPC concrete s fate attack [3-5], OFC [1, 2].

FTIR spectroscopy has become one of the most powerful techniques developed to be applied for molecular characterization. The principle of the infrared spectroscopy is briefly described as that in a system of phases every molecule or group of atoms with different geometry and immediate surroundings will distinctly absorb different wavelengths of infrared light. Therefore, the presences of both crystallite and amorphous materials can be apparently detected by using sole FTIR result. Actually, when the infrared light with a span of different wavelengths is used to irradiate the sample, some of wavelengths of the light will be absorbed by the certain ingredients of sample depending on the chemical composition of the sample [6, 7]. Initially, the application of FTIR was mainly established to study chemistry of cement powder and its hydration product [6-8] and supplementary cementitious materials in which part of original OPC was replaced by equivalent amount of pozzolanic materials or chemical additives [9, 10]. Nowadays, its application has been widened for advanced awareness of hydration process of green cementing binder such as alkali-activated various mixtures of pozzolanic materials developed to qualify the requirement of sustainability development for construction material as aforementioned.

Recently, the presence of a new SFC binder has become an innovative way for concrete industry to achieve a new standard of sustainability development [11]. Indeed, the SFC binder was reported to be used for manufacturing self-compacting concrete with excellent passing and filling capacity, high compressive strength sufficient for structural concrete, and superior durability in terms of aggressive attack. As such, making a further study on chemistry of hydration process of SFC binder is urgently needed to build the document used for developing other kinds of binder based on its mechanism of hydration. Although the traditional techniques such as scanning electron microscope (SEM) and X-ray diffraction (XRD) have been completely used for detecting hydration products of such SFC binder as reported in previous study [11], no study focusing on the application of alternative powerful technique, particularly FTIR to confirm such new result. In this study, the examination on microstructure of the SFC no-cement binder is completely reported by using sole Fourier transform inferred (FTIR) spectra of raw materials and hardened hydrated pastes. The significance of the current study is not only to confirm the contribution of SEM and XRD to studying chemistry of cement hydration but also to widen the application of FTIR for microstructural examination of such new SFC no-cement or strong alkali or either other new kind of binders produced in accordance with the hydration mechanism of the SFC binder.

2. Experimental program

2.1. Materials and mix proportions

In this investigation, GGBFSlow calcium fly ash (FFA), and CFBC fly ash (CFA) were used to fabricate the SFC binder. The physicochemical compositions of these raw materials are shown in Table 1.

Table 1. *Physicochemical properties of three by-product materials*

Properties	GGBFS	FFA	CFA
Specific gravity	2.90	2.17	2.70
Blaine fineness, cm^2/g	6000	-	3000
SiO_2, wt.%	34.90	58.33	5.22
Al_2O_3, wt.%	13.53	26.23	2.21
Fe_2O_3, wt.%	0.52	3.49	0.58
CaO, wt.%	41.47	5.72	56.80
MgO, wt.%	7.18	1.26	2.06
SO_3, wt.%	1.74	-	32.40
Na_2O, wt.%	-	0.27	-
K_2O, wt.%	-	0.48	-
TiO_2, wt.%	-	1.46	-
L.O.I, wt.%	-	2.76	-

In the previous study [11], the optimum amount of CFA was 15 wt. % to combine with the mixture of GGBFS and FFA. Therefore, a 15 wt.% CFA was also fixed in this study. The ratios of FFA to GGBFS of 0/100, 10/90, 30/70, and 50/50 in mass were used to optimize the ingredients of the SFC binder. The water to binder ratio (W/B) of 0.35 was fixed for all mix proportions. The mix proportions of the SFCpastes are described in Table 2

Table 2. *Mix proportions for no-cement SFC binder pastes (Unit: g)*

| Mixtures	GGBFS	FA	CFBC	Water
F00	1000	-	150	402.5
F10	900	100	150	402.5
F30	700	300	150	402.5
F50	500	500	150	402.5

2.2. Specimen preparation and test methods

The cubic specimens with dimensions of $50 \times 50 \times 50$ mm were cast for uniaxial compression test. After 24 h cured in the molds at ambient temperature, all paste specimens wereremoved and cured in air at 27±2 °C. The broken pieces of the compressed specimens were collected and used for the FTIR test after being immersed in alcohol for at least 7 days for stopped hydration. In this study, the FTIR tests in accordance with ASTM C494 [12] were conducted at ages of ages of 3, 7, 14, and 28 days of curing to estimate the effect of hydration time on microstructure of the paste specimens.

3. Results and discussions

3.1. Analysis on FTIR spectra of raw materials

The results of Fourier transform inferred (FTIR) of three solid wastes are shown in Figure 1. Accordingly, Figure 1 shows that the main vibration band was at around 960 cm^{-1} for GGBFS which was lower than about 1040 cm^{-1} for FFA, which are associated with the asymmetrical stretching vibration of terminal Si–O (υ_{as} Si–O) and bridge Si–O–Si/Si–O–Al (υ_{as} Si–O–Si/Si–O–Al) bonds, respectively. The different frequencies of such main absorption band illustrated the different glassy networks of these two raw materials. Actually, the result in

this study obviously indicated that the breaking energy of the Si–O and bridge Si–O–Si/Si–O–Al bonds in GGBFS is lower than that in FFA, which clearly implies that the GGBFS can be more easily activated in low to medium alkaline solution when compared with FFA in the similar alkaline concentration.
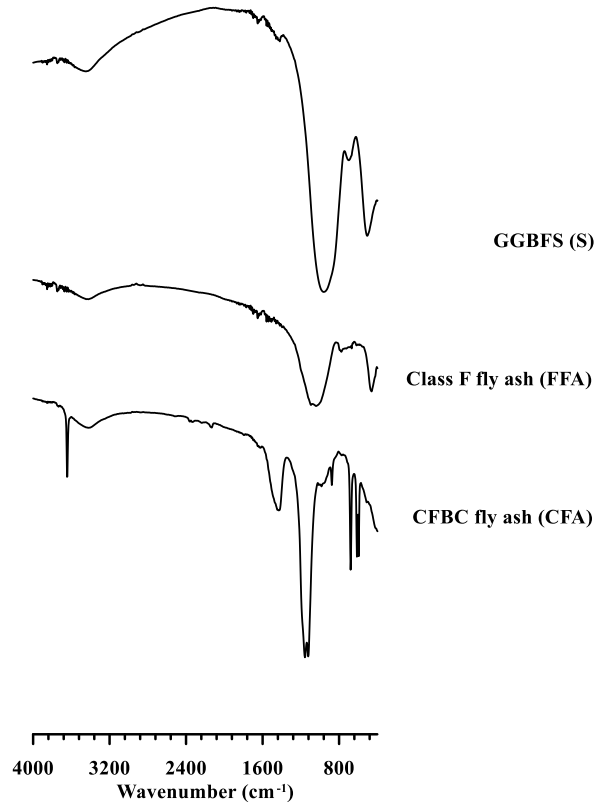
Figure 1. *FTIR spectra of three solid waste materials*

On the other hand, the feature of FTIR for CFA indicated the mostly presences of anhydrite ($CaSO_4$) and portlandite ($Ca(OH)_2$) transformed from the reaction of free lime (f-CaO) and vaporized water in air. Indeed, the information of $CaSO_4$ detected in FTIR spectrum of the CFA included a strong band centered around 1138 cm^{-1} splitting into two components at 1157 cm^{-1} and 1123 cm^{-1} and the sharp peaks at 679 and 613 cm^{-1} being assigned to the stretching and bending modes of sulfate. The sharp absorption band located at frequency of about 3645 cm^{-1} was assigned to the OH^- stretching in the $Ca(OH)_2$ crystals. The absorption band about 1423-1435 cm^{-1} was related to the asymmetric stretching vibration mode of unidentate carbonate anion group CO_3^{2-} (υ_{as} CO_3^{2-}) of carbonated CFA powder. Moreover, the absorption band at about 875 cm^{-1} illustrated a vibration of a bridging (out-of-plane bending) type CO_3^{2-} with $Ca(OH)_2$ lattice. The FTIR spectrum of CFA also showed the absorption bands at 3406-3425 and 1624 cm^{-1} which are respectively associated with the stretching and bending vibrations of O–H in absorbed H_2O linked to $Ca(OH)_2$ crystal. The observed portlandite and anhydrite in CFA makes it become alkali-sulfate activator of the SFC powder as contacting with distilled water. As aforementioned, the results in this study have totally confirmed the obtained results examined by XRD patterns reported in the previous study [11].

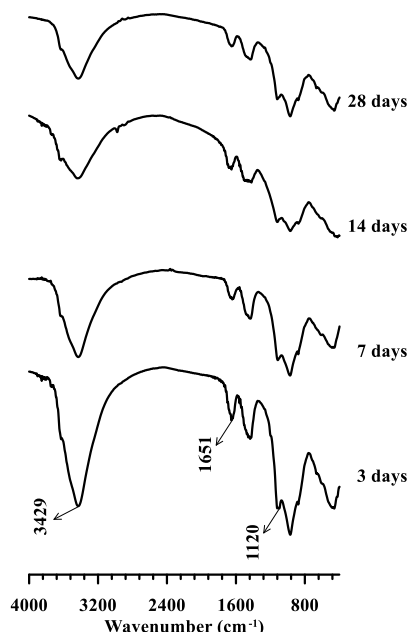## 3.2. Analysis on FTIR spectra hardened SFC paste

Figure 2(a). *FTIR spectra for F10 SFC binder with FFA/(FFA + GGBFS) = 10 wt.%*
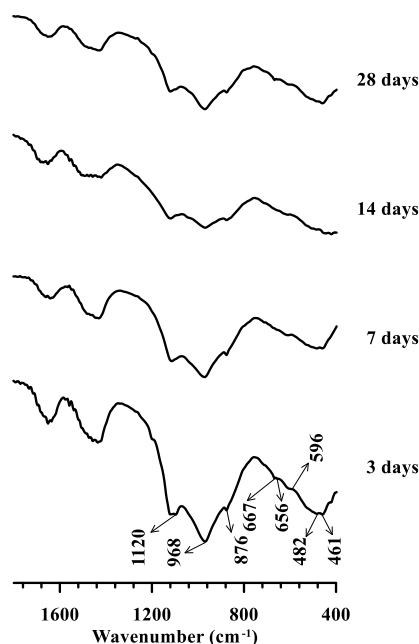

Figure 2(b). *FTIR spectra for F10 SFC binder with FFA/(FFA + GGBFS) = 10 wt.%*

The FTIR spectra of hydrated SFC binders are shown in Figures 2-3. The differences of FTIR spectra of the SFC binders, as shown in Figures 2-3, from those observed for the raw materials apparently proved for the hydration process of their mixture with distilled water. As can be seen in Figures 2-3, the vibrating spectrums of the SFC binders obviously imply the strongly precipitation of ettringite (AFt) crystals.

Indeed, the infrared spectra of such ettringite (AFt) illustrated a strong asymmetrical stretching frequency of the sulphate ion (υ_{as} SO$_4$) centered towards around 1120 cm^{-1}. Such vibrating band indicated a relative isolation of this ion

in the structure of AFt crystals. The symmetrical deforming bands of water absorption (δ_s H$_2$O) appeared in the region 1600-1700 cm^{-1}, and the bands located at regions above 3000 cm^{-1} were assigned for the symmetrical stretching vibration of absorbed water (υ_s H$_2$O) and stretching vibration of free OH (υ OH) (3420 assigned to υ_s H$_2$O and 3635 cm^{-1} to υ OH free). The stretching bands of aluminate were near to 550 cm^{-1} due to stretching Al–O groups in AlO6 (υ AlO6) and 855 cm^{-1} due to the Al–O–H bending (δ Al–O–H). The results of FTIR for AFt as reported in this study obviously confirmed the commonly observed results. In addition, Figure 2(b) shows that the mid- and far-infrared vibrating spectrums of the SFC binders were practically illustrated to be similar to that observed for a C-A-S-H gel. Accordingly, the silicate vibration regions of such C-A-S-H spectra generally contain a characteristic set of bands centered at around 970 cm^{-1}. Such bands could be assigned to asymmetrical stretching vibrations of Si–O bonds of the Q^2 tetrahedra (υ_{as} Si–O–Si). The band at 811 cm^{-1} could be assigned to Si–O stretching of Q^1 tetrahedra, and the bands located at lower wavenumbers (at 670 cm^{-1}) assigned to deformation vibrations of Si–O–T (δ Si–O–T, where T is either Si or Al). The group of bands near 500 cm^{-1} due to internal deformation of SiO$_4$ tetrahedra were observed in this study. The observed bands at 1400–1500 and 875 cm^{-1} indicated the carbonation of tested samples. Therefore these spectra indicate structural characteristics similar to those representative of blending structures of AFt crystals and amorphous C-A-S-H gels.
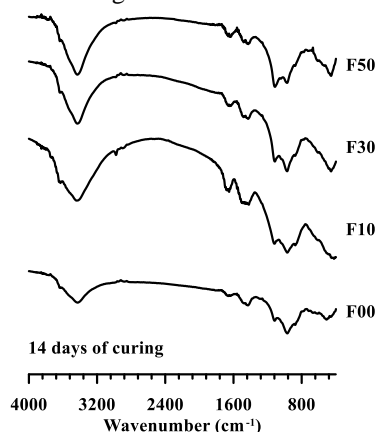

Figure 3. *Effect of FFA amount on FTIR spectra of SFC binders*

In this study, however, the observed FTIR spectra of SFC binders were not constant with the differentiated ages of curing and FFA addition. As shown in Figure 2, most of the intensities indicating the vibration bands of bonds between molecules precipitating both AFt crystals and C-A-S-H gels shifted toward the higher frequencies. Such result apparently showed an increased condensation of the hydration products with the increase of age of curing. The increase of FFA addition as partial replacement for GGBFS significantly changed the FTIR spectra of the hardened SFC binder. Figure 3 shows that, the increase of FFA to mixture of GGBFS and FFA ratio (FFA/(GGBFS +FFA)) from 0 to 50 wt.% increased the intensities assigned to the vibration bands (i.e. at 1120, 1600-1700, and above 3000 cm^{-1}) of the AFt crystals. This result could be explained according to the

increase of AFt formation contributed by the increase of active alumina with the increase of FFA addition because the FFA contains much more such ingredients than those of GGBFS [11]. As such, the increase of FFA additive played an important role in supplying the active alumina content for AFt precipitation during the hydration of SFC binder. Therefore, the observed FTIR in this study not only obviously contributed to confirming the reacting role of FFA in SFC hydration besides the filling effect but also apparently proved the goal of using FFA to optimize the chemical composition of the SFC binder by enriching the active alumina content in the main powder [11].

4. Conclusions

The application of Fourier transform infrared (FTIR) for microstructural examination of the SFC no-cement binder paste has been apparently reported. According to the experimental work obtained in this study, some of the following conclusions could be drawn:

• Circulating fluidized bed combustion (CFBC) fly ash mainly consists of portlandite ($Ca(OH)_2$) and anhydrite ($CaSO_4$) which act as alkali-sulfate activator pozzolanic materials such as ground granulated blast furnace slag and low calcium Class F fly ash and thus attributed to the hydraulic property of SFC powder.

• The main hydration products of the hardened SFC paste includes calcium aluminum silicate hydrate (C-A-S-H) gels and ettringite (AFt) crystals.

• An increase in FFA addition results in the higher degree of AFt precipitation because of an increase of active alumina in SFC mixture.

REFERENCES

[1] Juenger, M. C. G., Winnefeld, F., Provis, J. L., and Ideker, J. H. (2011). "Advances in alternative cementitious binders", Cement and Concrete Research, 41(12), 1232-1243.

[2] Damtoft, J. S., Lukasik, J., Herfort, D., Sorrentino, D., and Gartner, E. M. (2008). "Sustainable development and climate change initiatives", Cement and Concrete Research, 38(2), 115-127.

[3] Baghabra Al-Amoudi, O. S. (2002). "Attack on plain and blended cements exposed to aggressive sulfate environments", Cement and Concrete Composites, 24(3–4), 305-316.

[4] Bertron, A., Duchesne, J., and Escadeillas, G. (2005). "Attack of cement pastes exposed to organic acids in manure", Cement and Concrete Composites, 27(9–10), 898-909.

[5] Gruyaert, E., Van den Heede, P., Maes, M., and De Belie, N. (2012). "Investigation of the influence of blast-furnace slag on the resistance of concrete against organic acid or sulphate attack by means of accelerated degradation tests", Cement and Concrete Research, 42(1), 173-185.

[6] Mollah, M. Y. A., Yu, W., Schennach, R., and Cocke, D. L. (2000). "A Fourier transform infrared spectroscopic investigation of the early hydration of Portland cement and the influence of sodium lignosulfonate", Cement and Concrete Research, 30(2), 267-273.

[7] Ylmén, R., Jäglid, U., Steenari, B.-M., and Panas, I. (2009). "Early hydration and setting of Portland cement monitored by IR, SEM and Vicat techniques", Cement and Concrete Research, 39(5), 433-439.

[8] Hughes, T. L., Methven, C. M., Jones, T. G. J., Pelham, S. E., Fletcher, P., and Hall, C. (1995). "Determining cement composition by Fourier transform infrared spectroscopy", Advanced Cement Based Materials, 2(3), 91-104.

[9] Moraes, J. C. B., Akasaki, J. L., Melges, J. L. P., Monzó, J., Borrachero, M. V., Soriano, L., Payá, J., and Tashima, M. M. (2015). "Assessment of sugar cane straw ash (SCSA) as pozzolanic material in blended Portland cement: Microstructural characterization of pastes and mechanical strength of mortars", Construction and Building Materials, 94, 670-677.

[10] Brasileiro, G. A. M., Vieira, J. A. R., and Barreto, L. S. (2013). "Use of coir pith particles in composites with Portland cement", Journal of Environmental Management, 131, 228-238.

[11] Chen, C.-T., Nguyen, H.-A., Chang, T.-P., Yang, T.-R., and Nguyen, T.-D. (2015). "Performance and microstructural examination on composition of hardened paste with no-cement SFC binder", Construction and Building Materials, 76, 264-272.

[12] ASTM C494 (2017), American Standard Specification for Chemical Admixtures for Concrete.